Electronic Structure and Optical Properties of Ca(NH2BH3)2 Studied from GW Calculations

ARTICLE *in* THE JOURNAL OF PHYSICAL CHEMISTRY C · AUGUST 2011

Impact Factor: 4.77 · DOI: 10.1021/jp203798q

THE JOURNAL OF PHYSICAL CHEMISTRY C

ARTICLE

pubs.acs.org/JPCC

Electronic Structure and Optical Properties of $Ca(NH_2BH_3)_2$ Studied from GW Calculations

Ch. Bheema Lingam,[†] K. Ramesh Babu,[‡] Surya P. Tewari,[†,‡] G. Vaitheeswaran,[*,‡] and S. Lebègue[§]

[†]School of Physics and [‡]Advanced Centre of Research in High Energy Materials (ACRHEM), University of Hyderabad, Prof. C. R. Rao Road, Gachibowli, Andhra Pradesh, Hyderabad- 500 046, India

[§]Laboratoire de Cristallographie, Résonance Magnétique et Modélisations (CRM2, UMR CNRS 7036), Institut Jean Barriol, Nancy Université BP 239, Boulevard des Aiguillettes, 54506 Vandoeuvre-lès-Nancy, France

ABSTRACT: The quasiparticle band structure and optical properties of calcium amidoborane $Ca(NH_2BH_3)_2$ have been studied by means of the GW approximation based on the projected augmented wave(PAW) method. From the calculated band structure, $Ca(NH_2BH_3)_2$ is found to be an insulator with a bandgap of 3.27 eV within GGA and 6.12 eV within the GW approximation. The dielectric function corrected by a scissor shift operation corresponding to the GW correction on the GGA bandgap is computed to obtain the optical properties. The different peaks in the optical spectra are studied in terms of optical transitions within the calculated band structure. The optical anisotropy of this material is analyzed through refractive indices and the static dielectric constants along the three principle axes. It is found that $Ca(NH_2BH_3)_2$ system is optically less anisotropic than NH_3BH_3 due to similarities in the bonding along the *a* and *c* axes.

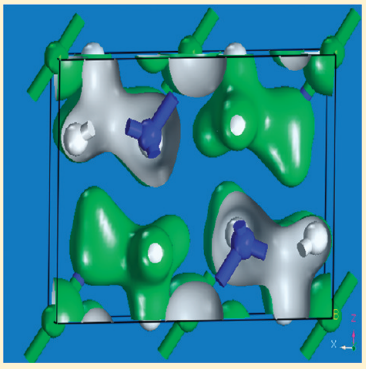

I. INTRODUCTION

Metal amidoboranes with accelerating desorption kinetics and suppressed toxic borazine are of great interest for their potential applications in hydrogen storage.[1,2] These are stable under normal pressures, less exothermic than NH_3BH_3, and suitable for on-board H_2-storage application.[1,2] Recently, $LiNH_2BH_3$, $NaNH_2BH_3$, and $Ca(NH_2BH_3)_2$ have been highlighted as potential materials[3] for hydrogen storage applications, because they release H_2 at ~363 K.[1,2] $LiNH_2BH_3$ and $Ca(NH_2BH_3)_2$ have been reported to show significantly enhanced dehydrogenation kinetics and suppressed borazine release. In this paper we focus on calcium amidoborane $Ca(NH_2BH_3)_2$, which is a new type of hydrogen storage material having 10.10 wt % of hydrogen content, with a monoclinic structure having the space group C2 ($Z = 2$) with lattice parameters $a = 9.100(2)$ Å, $b = 4.371(1)$ Å, $c = 6.441(2)$ Å, and $\beta = 93.19^o$. A combined X-ray diffraction and first principles study on the structure, crystal chemistry, and hydrogen storage properties of $Ca(NH_2BH_3)_2$ has been reported recently.[1] However, some of its fundamental properties such as the electronic structure and the optical properties have not been completely investigated. Therefore, considerable theoretical studies are still needed to understand the various physical properties of $Ca(NH_2BH_3)_2$ which are qualitatively different from that of other hydrides. For instance, photoemission, inverse photoemission, and VUV spectroscopy are important experimental tools to understand the electronic structure of materials, including the ones for hydrogen storage, and ab initio calculations are able to provide similar information, either to comfort experiments afterward or to be predictive. Moreover, during recent years,[4,5] hydrogen storage materials in the form of thin films gained considerable attention by the scientists around the globe because of their peculiar optical properties that makes these materials to find applications as switchable mirrors. The notable characteristic of these switchable mirrors is that they can be switched continuously or reversibly between metallic reflecting states to an insulating transparent state by the absorption of hydrogen on the metal thin film. An other important application of hydrogen rich materials is that they can serve as smart optical windows with considerable transparency. Moreover the variation in optical properties with the hydrogen concentration on thin films can also be useful as an indicator for hydrogen storage. A technique known as hydrogenography (see refs 6 and 7) is using the fact that the optical properties of hydrogen materials are strongly modified when hydrogen is incorporated or desorbed to measure the thermodynamics of the corresponding reaction. The importance of having corresponding ab initio calculations has been highlighted again recently in ref 8. To the best of our knowledge, some basic questions about the properties of $Ca(NH_2BH_3)_2$ are still unsolved, such as (i) the detailed electronic structure and the corresponding excited-state properties and (ii) the anisotropic optical behavior. Answers to these questions lead to the knowledge of the value of the band gap and its direct/indirect nature as well as the optical properties which are extremely important for

Received: April 24, 2011
Revised: August 12, 2011
Published: August 15, 2011

dx.doi.org/10.1021/jp203798q | *J. Phys. Chem. C* 2011, 115, 18795–18801

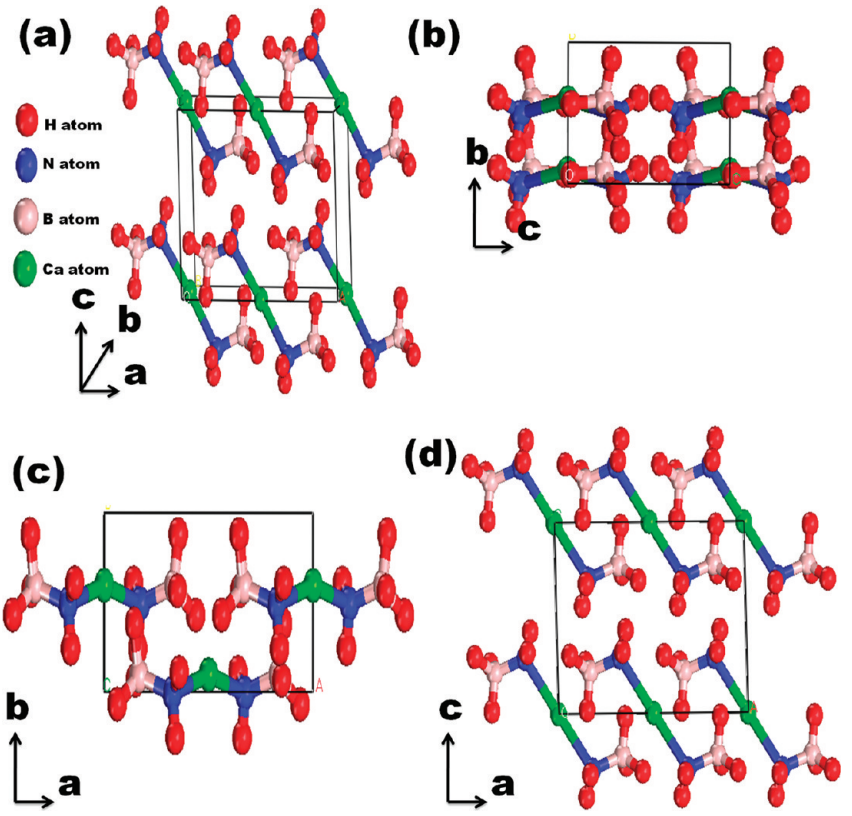

Figure 1. (a) Crystal structure of monoclinic $Ca(NH_2BH_3)_2$. The corresponding structure is represented along crystallographic directions (b) along *a* axis, (c) along *c* axis, and (d) along *b* axis.

hydrogen release applications. However, the results concerning the electronic structure and the optical properties are subject to caution due to the well-known problem of the density functional theory (DFT) to deal with excited states.[9] The GW approximation, where the quasiparticle self-energy is approximated as the product of the Green function G and the screened Coulomb interaction W, is a tool of choice for computing the excited states of materials. Therefore, in this study, we have investigated the excited-state properties of $Ca(NH_2BH_3)_2$ by calculating the quasiparticle bandstructure using GW approximation. Our paper is organized as follows: in the next section, we briefly discuss the computational details, then we present the quasiparticle (QP) band structure as well as the dielectric function and the related optical properties and, finally we summarize and conclude our paper.

II. COMPUTATIONAL DETAILS

The ground state properties of $Ca(NH_2BH_3)_2$ were calculated using a plane wave basis in the frame of density functional theory as implemented in the CASTEP code.[10] We have used Vanderbilt-type ultrasoft pseudo potentials[11] for describing the electron-ion interactions. The structures were relaxed using the Broyden, Fletcher, Goldfarb, and Shannon (BFGS) method.[12] The exchange-correlation potential of Ceperley and Alder[13] as parametrized by Perdew and Zunger[14] in the local density approximation (LDA) and also the generalized gradient approximation (GGA) with the Perdew-Burke-Ernzerhof (PBE) parametrization[15] was used to describe the electron−electron interactions. The valence electrons are $3s^2$, $3p^6$, $4s^2$ for calcium, $2s^2$,$2p^3$ for nitrogen, $2s^2$,$2p^1$ for boron, and $1s^1$ for hydrogen. A plane wave basis set with an energy cutoff of 500 eV has been used. For the Brillouin zone sampling, a $5 \times 6 \times 5$ Monkhorst-Pack[16] mesh has been used, and at the end of the relaxation, the remaining forces on the atoms are less than 0.0005 eV/Å.

Since DFT has difficulties to treat the excited states, and in particular, the band gap, which is usually underestimated by standard functionals like the LDA or the GGA, we have used the GW approximation (GWA)[17,18] to obtain the quasiparticle bandstructure of $Ca(NH_2BH_3)_2$. Instead of the Kohn−Sham equations used in DFT, the following quasiparticle equation is used:

$$(T + V_{\text{ext}} + V_{\text{h}})\psi_{\mathbf{k}n}(\mathbf{r}) + \int \mathrm{d}^3r'\, \Sigma(\mathbf{r}, \mathbf{r}', E_n(\mathbf{k}))\psi_{\mathbf{k}n}(\mathbf{r}') = E_n(\mathbf{k})\psi_{\mathbf{k}n}(\mathbf{r}) \quad (1)$$

here T is the kinetic energy operator, V_{ext} is the external potential from the ion cores, and V_h is the Hartree potential, Σ is the self-energy operator, and $E_n(\mathbf{k})$ and $\psi_{\mathbf{k}n}(\mathbf{r})$ are respectively the quasiparticle energy and quasiparticle wave function. Then, Σ is approximated (the vertex corrections are neglected) as the product of the Green's function G times the screened Coulomb interaction W. In practice, the GW quasiparticle eigenvalues are calculated as a correction to the DFT eigenvalues $\epsilon_n(\mathbf{k})$ like[19]

$$ReE_n(\mathbf{k}) = \epsilon_n^{\text{DFT}}(\mathbf{k}) + Z_{n\mathbf{k}} \times [\langle \Psi_{\mathbf{k}n}^{\text{DFT}} | Re\Sigma(\mathbf{r}, \mathbf{r}', \epsilon_n(\mathbf{k})) | \Psi_{\mathbf{k}n}^{\text{DFT}} \rangle - \langle \Psi_{\mathbf{k}n}^{\text{DFT}} | V_{xc}^{\text{DFT}}(r) | \Psi_{\mathbf{k}n}^{\text{DFT}} \rangle] \quad (2)$$

dx.doi.org/10.1021/jp203798q |J. Phys. Chem. C 2011, 115, 18795–18801

Table 1. Internal Coordinates of $Ca(NH_2BH_3)_2$ Calculated using CASTEP

atom	method	x	y	z
B	LDA	0.831	0.089	0.780
	GGA	0.833	0.077	0.797
	other[a]	0.832	0.032	0.790
	expt[a]	0.835(2)	0.064(3)	0.815(4)
N	LDA	0.672	0.993	0.708
	GGA	0.672	1.011	0.734
	other[a]	0.670	0.957	0.723
	expt[a]	0.675(2)	0.024(1)	0.725(3)
H1	LDA	0.936	0.930	0.696
	GGA	0.856	1.050	0.983
	other[a]	0.924	0.873	0.705
	expt[a]	0.926	0.922	0.715
H2	LDA	0.146	0.380	0.266
	GGA	0.137	0.340	0.248
	other[a]	0.141	0.299	0.255
	expt[a]	0.145	0.344	0.212
H3	LDA	0.850	0.064	0.981
	GGA	0.856	0.050	0.983
	other[a]	0.855	0.005	0.982
	expt[a]	0.861	0.008	0.003
H4	LDA	0.638	0.108	0.564
	GGA	0.642	0.122	0.602
	other[a]	0.639	0.066	0.586
	expt[a]	0.653	0.162	0.598
H5	LDA	0.341	0.742	0.321
	GGA	0.345	0.803	0.320
	other[a]	0.343	0.729	0.309
	expt[a]	0.345	0.803	0.320
Ca	LDA	0	0.595	0
	GGA	0	0.609	0
	other[a]	0	0.557	0
	expt[a]	0	0.560(3)	0

[a] Reference 1.

with the QP renormalization factor $Z_{n\mathbf{k}}$ being

$$Z_{n\mathbf{k}}^{\mathrm{DFT}} = \left[1 - \langle \Psi_{\mathbf{k}n}^{\mathrm{DFT}} | \frac{\partial}{\partial \omega} Re\Sigma(\mathbf{r}, \mathbf{r}', \epsilon_n(\mathbf{k})) | \Psi_{\mathbf{k}n}^{\mathrm{DFT}} \rangle\right]^{-1}$$

We have used the implementation of the GW approximation provided by the code VASP (Vienna ab-initio simulation package),[20] which gives essentially similar results as an earlier implementation[21,22] of the GW approximation within the PAW framework. To reach convergence, we used 200 bands for the summation over the bands in the polarizability and the self-energy formulas, and the polarizability matrices were calculated up to a cutoff of 250 eV. Then, we obtained the optical properties as outlined in refs 23 and 24.

III. RESULTS AND DISCUSSION

A. Electronic Properties. The monoclinic cell of $Ca(NH_2BH_3)_2$ considered in the present work is shown in Figure 1. Its space group is *C*2, and this structure contains two formula units, i.e., two calcium atoms, four boron atoms, and four nitrogen atoms per cell. Each boron atom is surrounded by three hydrogen atoms, whereas each nitrogen atom is surrounded by two hydrogen atoms. The distinct feature is that the two units NH_2BH_3 are connected through Ca atom. The Ca sites are at middle of the *b* and *a* axes, the two NH_2BH_3 units are stretched in the ab-plane. We have optimized the monoclinic structure of $Ca(NH_2BH_3)_2$ using CASTEP within LDA and GGA. The calculated ground-state properties such as equilibrium lattice constants within LDA (GGA) are a = 8.820 (9.263) Å, b = 4.043 (4.424) Å, c = 6.175 (6.628) Å, and β = 91.61 (93.13)° are in reasonable agreement with the experiments.[1] The calculated atomic positions of each atom are compared with the experimental and the other theoretical values are shown in Table 1. Since $Ca(NH_2BH_3)_2$ is a molecular crystal, the van der Waals (vdW) long-range dispersion forces might play an important role. Then, we have also optimized the $Ca(NH_2BH_3)_2$ crystal structure with PBE+D2 (Grimme's correction) to treat the vdW long-range dispersion forces as implemented in CASTEP[25] and VASP.[26] In this case, the ground state lattice parameters with VASP (CASTEP) are a = 8.905 (8.922) Å, b = 4.147 (4.140) Å, c = 6.276 (6.293) Å, and β = 91.21 (91.26)°. Therefore, the unit cell volume obtained by LDA is underestimated by 13.9% and with GGA it is overestimated by 6.0%, whereas with vdW corrections (PBE+D2) it is underestimated by 9.1%. Therefore, the correction brought by the PBE+D2 scheme appears to be too strong in the case of $Ca(NH_2BH_3)_2$, a fact that we have already noticed in our previous work[26] using the PBE+D2 method. Also, the corresponding

Table 2. Internal Coordinates of $Ca(NH_2BH_3)_2$ Calculated with vdW Correction (PBE+D2) as Implemented in CASTEP and VASP

atom	method	x	y	z
B	VASP	0.828	0.091	0.776
	CASTEP	0.830	0.090	0.777
	expt[a]	0.835(2)	0.064(3)	0.815(4)
N	VASP	0.668	0.988	0.707
	CASTEP	0.670	0.990	0.709
	expt[a]	0.675(2)	0.024(1)	0.725(3)
H1	VASP	0.932	0.940	0.691
	CASTEP	0.932	0.937	0.692
	expt[a]	0.926	0.922	0.715
H2	VASP	0.154	0.377	0.267
	CASTEP	0.150	0.375	0.267
	expt[a]	0.145	0.344	0.212
H3	VASP	0.846	0.065	0.975
	CASTEP	0.849	0.064	0.974
	expt[a]	0.861	0.008	0.003
H4	VASP	0.636	0.098	0.568
	CASTEP	0.637	0.101	0.569
	expt[a]	0.653	0.162	0.598
H5	VASP	0.339	0.746	0.322
	CASTEP	0.339	0.746	0.318
	expt[a]	0.345	0.803	0.320
Ca	VASP	0	0.594	0
	CASTEP	0	0.600	0
	expt[a]	0	0.560(3)	0

[a] Reference 1.

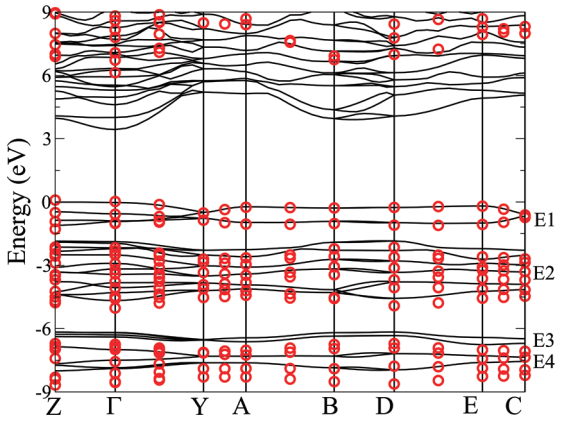

Figure 2. Bandstructure of $Ca(NH_2BH_3)_2$ calculated within GGA (black lines) and with GW approximation (red circles). The energy ranges in valence band defined as E1 = −1.5 to 0 eV (at Fermi level), E2 = −5 to −1.5 eV, E3 = -7 to −6 eV, and E4 = −8 to −7 eV.

atomic positions are compared with the experiments in Table 2, with a reasonable agreement with experiments.

The calculated band structure of $Ca(NH_2BH_3)_2$, which is qualitatively different from that of NH_3BH_3 (see ref 27), along the high symmetry directions in the Brillouin zone within GGA is shown in Figure 2 (black lines). From the band structure, the top of the valence band and the bottom of the conduction band occur at the Γ point with a band gap of 3.27 eV, indicating that $Ca(NH_2BH_3)_2$ is a direct bandgap insulator. However one has to use the GW approximation for a more correct calculation.[23] So, in order to treat excited states and to obtain a correct bandgap, GW calculations have been performed. The obtained band gap value is apparently enhanced by using the GW approximation when compared to the GGA value. In Figure 2, we present the GW band structure with circles on top of the GGA band structure. The minima found for the conduction band are as follows for GW (GGA): Z-point occurs at 6.96 eV (3.87 eV), Γ-point at 6.12 eV (3.27 eV), Y-point at 8.47 eV (5.19 eV), A-point at 8.09 eV (5.10 eV), B-point at 6.71 eV (3.90 eV), D-point at 7.05 eV (4.03 eV), E-point at 7.90 eV (4.85 eV), and C-point at 7.91 eV (5.01 eV), respectively. By using the GW approximation, the minimum direct band gap is observed at the Γ point with a value of 6.12 eV. In the band structure, the valence bands have essentially four regions, −1.5 to 0 eV, −5 to −1.5 eV, −7 to −6 eV, and −8 to −7 eV.

In order to clearly analyze the various atoms contribution, the corresponding charge density distributions along (100), (010) and (001) planes and corresponding partial density of states (PDOS) at different energy ranges in the valence band are plotted in Figure 3, for which the energy ranges are defined as E1 = −1.5 to 0 eV (the Fermi level), E2 = −5 to −1.5 eV, E3 = −7 to −6 eV, and E4 = −8 to −7 eV. From the plot, in the E1 energy region, the main states are the N 2p states. At the same time, a weak hybridization between B 2p states and H1 and H3 s states is also found in this energy region. In the E2 energy region, there is a strong hybridization between the 1s states of H1, H2, H3 atoms and 2p states of B, N respectively. The next region E3 displays a hybridization between N 2p and H4 and H5 s states, whereas the E4 energy region displays the hybridization between the B 2s and N 2p states. On the basis of the above discussions about the bandstructure and the charge density distribution, we find that $Ca(NH_2BH_3)_2$ forms covalent bonds between B atoms and its surrounding hydrogen (H1, H2, and H3) atoms, while bonds between N atoms and the surrounding hydrogen (H4 and H5) atoms are relatively weaker.

B. Optical Properties. Now, we focus our attention on the optical properties of $Ca(NH_2BH_3)_2$. Optical spectroscopy is an important tool for studying the electronic structure of materials and therefore precise ab initio calculations are needed to compute the optical spectra. Being a molecular crystal this material is also highly anisotropic from a structural point of view. However, as for as optical properties, this type of molecular crystal shows less anisotropy in their optical properties than in the structural properties.[23] The optical properties of matter can be described by means of the dielectric function $\epsilon(q,\omega)$ where q is the momentum and ω is the energy. In the present study we have used the dipole approximation for the calculations, i.e., $q = 0$, the momentum transfer from the initial state to the final state is neglected. In general, there are two contributions to $\epsilon(\omega)$ namely intraband and interband transitions: the contribution from intraband transitions is important only for the case of metals, and the interband transitions can be direct and indirect transitions. The indirect interband transitions involve scattering of phonons, but the indirect transitions give only a small contribution to $\epsilon(\omega)$ in comparison to the direct transitions,[24] so we have neglected them in our calculations. The direct interband contribution to the absorptive or imaginary part of the dielectric function $\epsilon(\omega)$ in the random phase approximation[28] without local field effects is calculated by summing all the possible transitions from the occupied and unoccupied states for a set of k-vectors over the first Brillouin zone. For the calculation of optical properties one needs a dense mesh, and hence the Brillouin zone integration was performed with a 13 × 16 × 14 k-points mesh. Then the real and imaginary parts of the dielectric function $\varepsilon(\omega)$ as a function of photon energy along three crystallographic ([100], [010], and [001]) directions have been calculated using CASTEP within GGA (see figure 4). A scissor operator correction of 2.85 eV has been applied in order to correct the deficiency of density functional theory (DFT) to deal with the band gap. The imaginary part of the dielectric function, $\varepsilon_2(\omega)$, has four prominent peaks at different photon energies in three crystallographic ([100], [010], and [001]) directions, which are due to the interband transitions between valence and conduction bands. The imaginary part $\varepsilon_2(\omega)$ exhibits a sharp increase at 6.48 eV in the [100] and [001]crystallographic directions and at 7.18 eV in the [010] direction, which is the threshold energy of the dielectric function of $Ca(NH_2BH_3)_2$. This corresponds to the transitions at the high symmetry point Γ between the highest valence and the lowest conduction bands (i.e., N 2p → Ca 3d), and it is known as the fundamental absorption edge. Around 7.64 eV, a peak appears only along the [001] direction, the origin of this peak being from N 2p → Ca 3d interband transitions. A sharp peak around 9.01 eV arises along the [100] and [001] directions, whereas it is absent in the [010] direction, the origin of this peak is from B 2p → Ca 3d interband transitions. A peak around 10.32 eV arises along [100] and [010] direction and originates from N or B 2p → Ca 3d interband transitions. A peak around 11.28 eV along the [010] and [001] directions is from N 2p → Ca 3d interband transitions. A peak around 13.29 eV appears in the [100] and [010] directions, from N 2p → Ca 3d interband transitions. The peak around 14.08 eV appears along the [001] and [010] directions. The origin of this peak might be from the B 2p → Ca 3d interband transitions. It is noted that a peak in $\varepsilon_2(\omega)$ does not correspond to a single interband transition since many transitions can be found in the

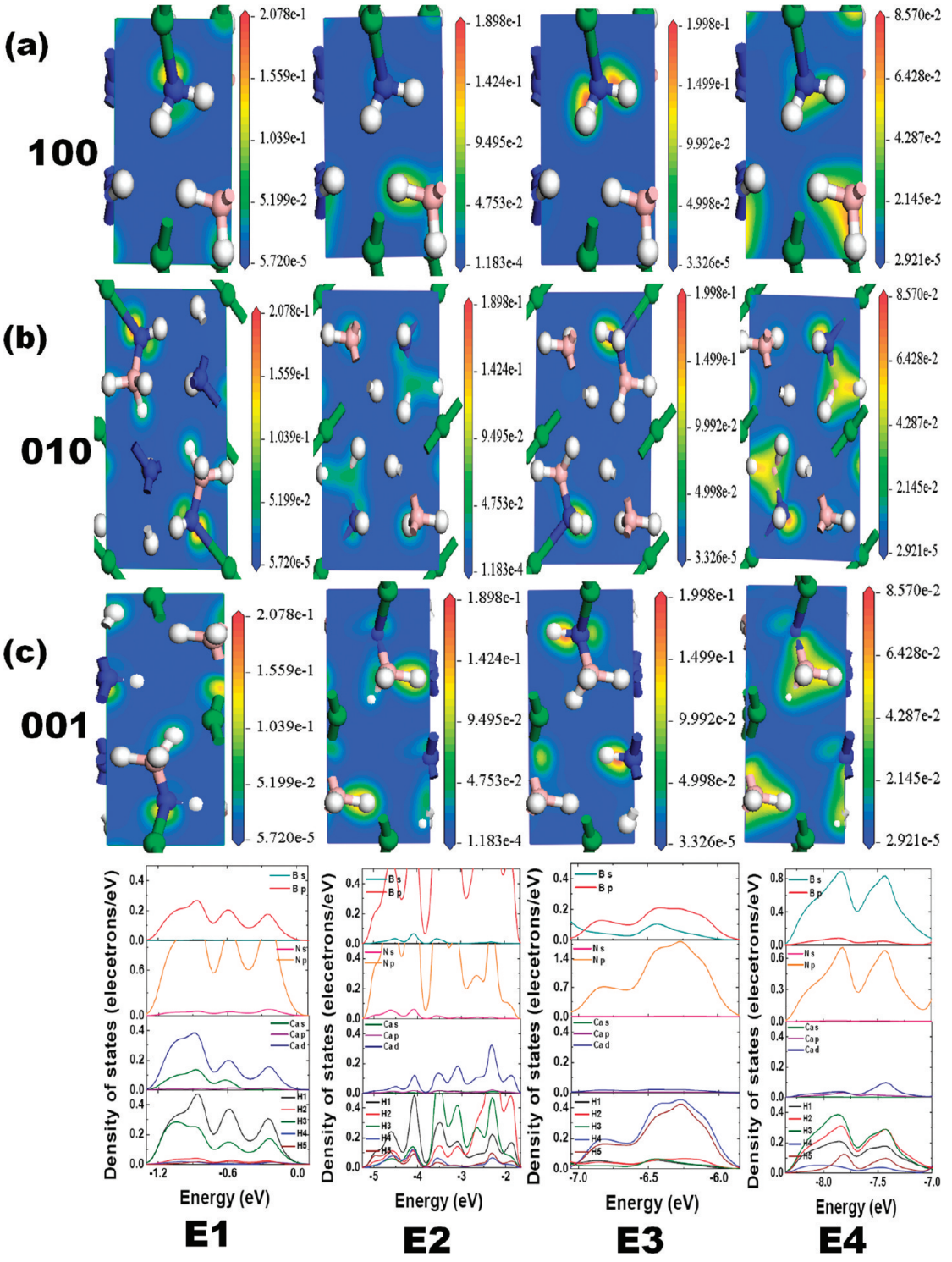

Figure 3. Charge density distribution plots (a) along the *a* axis, (b) along the *b* axis, and (c) along the *c* axis and along with corresponding partial density of states (PDOS) are shown for different energy ranges in valence band defined as E1 = −1.5 to 0 eV (at Fermi level), E2 = −5 to −1.5 eV, E3 = −7 to −6 eV, and E4 = −8 to −7 eV.

band structure with the energy corresponding to the same peak. The real part $\varepsilon_1(\omega)$ of the dielectric function is evaluated from the calculated imaginary part $\varepsilon_2(\omega)$ by using Kramer's-Kronig relations (see figure 4). The static real part of dielectric function, $\varepsilon_1(0)$ along three crystallographic directions are found to be 2.02 (along [100]), 2.20 (along [010]), and 2.10 (along [001]).

Further, using $\varepsilon_1(\omega)$ and $\varepsilon_2(\omega)$, we evaluated the related optical properties, namely the refractive index $n(\omega)$, the reflectivity $R(\omega)$, and the energy-loss spectrum $L(\omega)$ (see Figure 4). The peaks in each of these spectra correspond to the peaks observed in the imaginary part $\varepsilon_2(\omega)$ of dielectric function. The refractive index of a crystal is closely related to the electronic

dx.doi.org/10.1021/jp203798q |*J. Phys. Chem. C* 2011, 115, 18795–18801

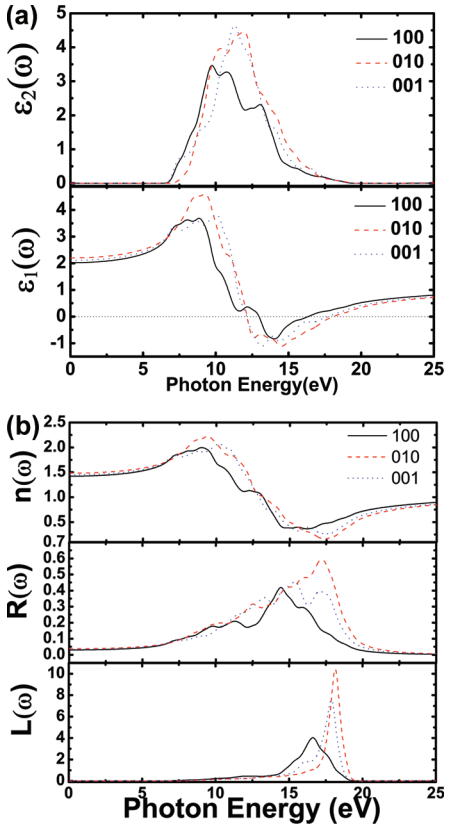

Figure 4. (a) Real ($\varepsilon_1(\omega)$) and imaginary ($\varepsilon_2(\omega)$) parts of the dielectric function and (b) the refractive index ($n(\omega)$), reflectivity ($R(\omega)$), and loss function ($L(\omega)$) of $Ca(NH_2BH_3)_2$ calculated within GGA at the theoretical equilibrium volume, with a scissor's shift of 2.85 eV.

polarizability of ions and the local field inside the crystal. The values of $n(0)$ along three crystal directions are found to be 1.42 (along [100]), 1.48 (along [010]), and 1.45 (along [001]). This clearly indicates the low optical anisotropy of $Ca(NH_2BH_3)_2$. The reflectivity spectrum $R(\omega)$ of $Ca(NH_2BH_3)_2$ along three crystal directions is calculated. The values of $R(0)$ are 0.030 (along [100]), 0.037 (along [010]), and 0.033 (along [001]). Below 7 eV of incoming photon energy, the compound has an isotropic behavior and but above that energy it has considerable anisotropy. The most prominent peaks are observed at 14.45, 17.20, and 15.36 eV along the three crystal directions [100], [010], and [001] respectively. The energy-loss function is calculated and shown in Figure 4. It is an important optical parameter, indicating the energy loss of a fast electron traversing in the material. The peaks represent the characteristic behaviors associated with the plasma oscillations and the corresponding frequencies are the so-called plasma frequencies. The peaks of $L(\omega)$ correspond to the trailing edges in the reflection spectra and are observed at around 16.62 eV (along [100]), 18.14 eV (along [010]), and 17.88 eV (along [001]). Overall, from the comparison of the optical properties of $Ca(NH_2BH_3)_2$ and NH_3BH_3,[23] the addition of an alkaline earth metal atom to NH_3BH_3 renders the system less optically anisotropic with respect to NH_3BH_3, which is related to the difference in the electronic structure induced by the presence of the extra calcium atom in $Ca(NH_2BH_3)_2$.

IV. CONCLUSION

In conclusion, we optimized the crystal structure of $Ca(NH_2BH_3)_2$ using CASTEP and compared our calculated values to experiments. Then, we have used the GW approximation implemented in VASP to obtain the band gap and presented the quasiparticle band structure and optical properties of $Ca(NH_2BH_3)_2$. From the band structure it is found that the band gap value is 3.27 eV with GGA and 6.12 eV with the GW approximation, and it occurs at the Γ high symmetry point. The calculated dielectric function and refractive index along the three crystallographic directions indicates that the optical anisotropy in $Ca(NH_2BH_3)_2$ is low compared to NH_3BH_3. From the loss function, we find that $Ca(NH_2BH_3)_2$ becomes transparent for frequencies above 17.90 eV. The calculated reflectivity spectrum is isotropic up to an energy of about 7 eV and for high energies a clear anisotropy is observed. The maximum reflection occurs at energy of about 13, 15, and 17 eV along the [100], [010], and [001] directions respectively. Moreover, we hope that our study will stimulate further experiments on $Ca(NH_2BH_3)_2$.

AUTHOR INFORMATION

Corresponding Author
*E-mail: gvsp@uohyd.ernet.in.

ACKNOWLEDGMENT

Ch.B.L. thanks CAS-RFSMS and K.R.B. thanks DRDO through ACRHEM for the financial support. Ch.B.L. and K.R.B. thank CMSD, University of Hyderabad for computational time. Supercomputer time was provided by GENCI (Project x2010085106). S.L. acknowledges financial support from ANR Grant No. ANR-06-NANO-053−02 and ANR Grant ANR-BLAN07-1-186138.

REFERENCES

(1) Wu, H; Zhou, W; Yildirim, T. *J. Am. Chem. Soc.* **2008**, *130*, 14834–14839.
(2) Kim, D. Y; Lee, H. M; Seo, J; Shin, S. K; Kim, K. S. *Phys. Chem. Chem. Phys.* **2010**, *12*, 5446–5453.
(3) Ramzan, M.; Silvearv, F.; Blomqvist, A.; Scheicher, R. H.; Lebègue, S.; Ahuja, R. *Phys. Rev. B* **2009**, *79*, 132102.
(4) Huiberts, J. N.; Griessen, R.; Rector, J. H.; Wijingarden, R. J. *Nature* **1996**, *380*, 231–234.
(5) Sandrock, G. A *J. Alloys. Compds.* **1999**, *293−295*, 877–888.
(6) Gremaud, R.; Broedersz, C. P.; Borsa, D. M.; Borgschulte, A.; Mauron, P.; Schreuders, H.; Rector, J. H.; Dam, B.; Griessen, R *Adv. Mater.* **2007**, *19*, 2813–2817.
(7) Gremaud, R.; Slaman, M.; Schreuders, H.; Dam, B.; Griessen, R. *App. Phys. Lett.* **2007**, *91*, 231916.
(8) van Setten, M. J.; Gremaud, R.; Brocks, G.; Dam, B.; Kresse, G.; de Wijs, G. A *Phys. Rev. B* **2011**, *83*, 035422.
(9) Fiorentini, V; Baldereschi, A. *Phys. Rev. B* **1995**, *51*, 17196–17198.
(10) Segall, M. D; Lindan, P. J. D; Probert, M. J; Pickard, C. J; Hasnip, P. J; Clark, S. J; Payne, M. C. *J. Phys.: Condens. Matter* **2002**, *14*, 2717–2744.
(11) Vanderbilt, D. *Phys. Rev. B* **1990**, *41*, 7892–7895.
(12) Fischer, T. H; Almolf, J. *J. Phys. Chem.* **1992**, *96*, 9768–9774.
(13) Ceperley, D. M; Alder, B. J. *Phys. Rev. Lett.* **1980**, *45*, 566–569.
(14) Perdew, J. P; Zunger, A. *Phys. Rev. B* **1981**, *23*, 5048–5079.
(15) Perdew, J. P.; Burke, K.; Ernzerhof, M. *Phys. Rev. Lett.* **1996**, *77*, 3865–3868.
(16) Monkhorst, H. J; Pack, J. D. *Phys. Rev. B* **1976**, *13*, 5188–5192.

(17) Hedin, L. *Phys. Rev.* **1965**, *139*, A796–A823.
(18) Hedin, L.; Lundquist, S. *Solid State Physics*; Academic: New York, 1969; Vol. 23, p 1.
(19) Onida, G; Reining, L; Rubio, A. *Rev. Mod. Phys.* **2002**, *74*, 601–659.
(20) Shishkin, M; Kresse, G. *Phys. Rev. B* **2006**, *74*, 035101.
(21) Lebègue, S; Arnaud, B; Alouani, M; Blöchl, P. E. *Phys. Rev. B* **2003**, *67*, 155208.
(22) Lebègue, S; Arnaud, B.; Alouani, M *Phys. Rev. B* **2005**, *72*, 085103.
(23) Bheema Lingam, Ch; Ramesh Babu, K; Tewari, S. P; Vaitheeswaran, G; Lebègue, S. *Phys. Status Solidi RRL* **2011**, *5*, 10–12.
(24) Ramesh Babu, K; Bheema Lingam, Ch; Auluck, S; Tewari, S. P; Vaitheeswaran, G. *J. Solid State Chem.* **2011**, *184*, 343–350.
(25) Grimme, S. *J. Comput. Chem.* **2006**, *27*, 1787–1799.
(26) Bučko, T; Hafner, J; Lebègue, S; Ángyán, J. G. *J. Phys. Chem. A* **2010**, *114*, 11814–11824.
(27) Bheema Lingam, Ch; Ramesh Babu, K; Tewari, S. P; Vaitheeswaran, G. *J. Comput. Chem.* **2011**, *32*, 1734–1742.
(28) Ehrenreich, H; Cohen, M. H. *Phys. Rev.* **1959**, *115*, 786–790.